Progress In Electromagnetics Research B, Vol. 36, 303–321, 2012

ASSESSMENT OF L-BAND SAR DATA AT DIFFERENT POLARIZATION COMBINATIONS FOR CROP AND OTHER LANDUSE CLASSIFICATION

D. Haldar[1, *], A. Das[1], S. Mohan[1], O. Pal[2], R. S. Hooda[2], and M. Chakraborty[1]

[1]Space Applications Centre, Indian Space Research Organization (ISRO), Ahmedabad 380015, India

[2]Haryana State Remote Sensing Applications Centre, Hisar, Haryana, India

Abstract—In the present study evaluation of L-band SAR data at different polarization combinations in linear, circular as well as hybrid polarimetric imaging modes for crop and other landuse classifications has been carried out. Full-polarimetric radar data contains all the scattering information for any arbitrary polarization state, hence data of any combination of transmit and receive polarizations can be synthesized, mathematically from full-polarimetric data. Circular and various modes of hybrid polarimetric data (where the transmitter polarization is either circular or orientated at 45°, called $\pi/4$ and the receivers are at horizontal and vertical polarizations with respect to the radar line of sight) were synthesized (simulated) from ALOS-PALSAR fullpolarimetric data of 14th December 2008 over central state farm central latitude and longitude 29°15′N/75°43′E and bounds for northwest corner is 29°24′N/75°37′E and southeast corner is 29°07′N/75°48′E in Hisar, Haryana (India) Supervised classification was conducted for crops and few other landuse classes based on ground truth measurements using maximum-likelihood distance measures derived from the complex Wishart distribution of SAR data at various polarization combinations. It has been observed that linear full-polarimetric data showed maximum classification accuracy (92%) followed by circular-full (89%) and circular-dual polarimetric data (87%), which was followed by hybrid polarimetric data (73–75%) and then linear dual polarimetric data (63–71%). Among the linear dual polarimetric data, co-polarization complex data showed better

Received 11 July 2011, Accepted 2 November 2011, Scheduled 16 November 2011

* Corresponding author: Dipanwita Haldar (dipanwita@sac.isro.gov.in).

classification accuracy than the cross-polarization data. Also multi-date single polarization SAR data over central state farm during *rabi* (winter) season was analyzed and it was observed that single date full-polarimetric SAR data produced equally good classification result as the multi-date single polarization SAR data.

1. INTRODUCTION

Synthetic Aperture Radar (SAR) data has shown promising results in crop discrimination and classification with reasonably high accuracy. Traditionally, crop classifications are done using multi-date SAR data that uses phenological information of crops to discriminate them. Single-date multi-polarization SAR data also has the potential to identify crops based on the variation in their scattering signatures in different polarizations. Various authors have reported of achieving significant classification accuracies for crops and other landuse classes using dual and quad polarimetric data from airborne as well as spaceborne SARs [1, 6, 7, 23, 24, 26]. Although there is a consensus that full-polarimetric imaging modes provide higher classification accuracies than dual polarimetric modes, opinions vary regarding the classification accuracies obtained by different modes of dual polarimetric SARs, including hybrid-dual polarimetric imaging modes. In this paper, evaluation of the performances of various single, dual and quad polarimetric SAR data in linear, circular and hybrid imaging modes in terms of their ability to discriminate and classify crops vis-a vis few other landuse classes was made.

Fullpolarimetric SAR systems collect complete polarimetric scattering information, at every imaged pixel. The standard implementation of fullpolarimetric SAR involves the coherent transmission and reception of both vertically (V) and horizontally (H) polarized radar pulses. Coherent collection of the fullpolarimetric scattering matrix in the H and V basis mathematically allows synthesis of any combination of transmit and receive polarizations. The dual polarization imaging modes simply do away with one of the transmitted polarizations, either H or V, but coherently receive both H and V backscattered polarizations. This helps achieving better range resolution; wider swath and reduces the data processing requirements compared to the full-polarimetric mode. But it also reduces the per-pixel information content in dual-polarization data [1]. In recent times a concept of hybrid-dual polarization imaging mode is gaining momentum where the transmission polarization is either 'circular' (called CTLR mode) or linear rotated by 45° with respect to H or V (called $\pi/4$ mode), while the received polarizations are coherent H

and V [1, 19, 21, 22, 25, 26]. These imaging modes, apart from having the advantages of standard dual-polarization modes, are also capable of retaining the complete polarimetric information of azimuthally symmetric targets pertaining to the backscattered field. Hence these imaging modes are superior to the standard dual polarimetric modes and often referred to as 'pseudo quad-polarization' modes. So far various planetary mission SARs have been operated in hybrid polarimetric modes and ISRO's RISAT-1 is going be the first earth observation space-borne SAR to incorporate the hybrid CTLR mode along with other modes of operation. An interesting aspect of the hybrid polarization imaging modes, the CTLR and $\pi/4$ modes, is the possibility of extending their applicability by incorporating the data into a polarimetric scattering model [1, 16, 26, 27], which leads to the descriptive name 'compact polarimetry' for both the CTLR and $\pi/4$ imaging modes. On the basis of symmetry properties of geophysical media, Lavalle et al. [9] proposed a reconstruction algorithm of the full-polarimetric information from a compact polarimetric dataset. The algorithm allows the assessment of compact POLINSAR and the comparison between the two compact configurations. Forested areas interferometric degree of coherence measured at different polarisations by compact polarimetry and full polarimetry has been compared. Recently a study focused on crops like winter wheat, maize and rape crops, and the biophysical parameters like crop coverage, Leaf Area Index (LAI), wet biomass and crop height. Time series of these polarimetric indicators and their relationship to crop development parameters and phenological stages have been analyzed by Ballester-Berman and Lopez-Sanchez [3]. Potential of some of these observables for both the detection of particular crop conditions and for continuous crop monitoring has been demonstrated. Also a preliminary analysis on the potential of hybrid-pol architecture decomposition parameters for agricultural monitoring and time series of such parameters has been studied.

Assessment of crop classification using 3-date HH polarization data used conventionally in most of the operational large area crop monitoring was compared with single-date dual, quad and hybrid-dual polarimetric modes. To address these questions the steps needed to reduce fullpolarimetric data to various dual-polarization data in linear, circular and hybrid imaging modes, have been discussed. Finally, the classification accuracies obtained were compared through these data with reference to ground truth measurements for *rabi* crops and few associated landuse classes. For these comparisons, we selected Central State farm, Hisar, India and its surroundings. ALOS-PALSAR L-band single, dual and fullpolarimetric data were used for the study.

Currently in another study authors have examined a time series analysis of various biophysical parameters like ground coverage, LAI, plant height, wet biomass for the *rabi* crops using both C-band and L-band SAR.

2. STUDY AREA AND DATASETS

Central State Farm located in Hisar, Haryana (India) has been selected for the present study. The area lies between 29°11′–29°20′N latitudes and 75°36′–75°45′E longitudes. This is a farmland of considerable size where large experimental crop fields are maintained for seed generation and distribution to the state farmers. The major agricultural crops grown in this area include paddy, maize, cotton and pulses during *kharif* (summer) and wheat, sugarcane, mustard, gram, peas during *rabi* (winter) seasons. This site was selected for developing methodology for crop discrimination and classification using data of various polarimetric modes synthesized from ALOS PALSAR polarimetric data.

Single-look complex (SLC) data of ALOS PALSAR L-band SAR have been used in the present study. The data were provided by Japan Aerospace Exploration Agency (JAXA) under an announcement of opportunity (A.O.) project carried out at SAC, India. In SLC data, each resolution cell of the image, called pixel is characterized by amplitude value (represents the strength of the returned signal) and an absolute phase value (represents the time delay of the received signal in a coherent system), both are jointly represented as a 'complex number'. Three-date HH polarization data (FBS) acquired on Jan. 02, Jan. 19 and Feb. 17, 2009 and one full-polarimetric data acquired on Dec. 14 2008 were used in the present study Details of these data are given in Table 1 below. The FBS data has been resampled to

Table 1. Details of ALOS-PALSAR data used in this study.

Sl. No.	Polarization	Central Inc. Angle	Acquisition Mode	Ground Range Pixel spacing	Date of Acquisition: DD/MM/YYYY
1	Quad (PLR)	23.1°	Ascending / right looking	~25m	14/12/2008
2	*HH* (FBS)	34.3°	Ascending / right looking	12m	02/01/2009
3	*HH* (FBS)	34.3°	Ascending / right looking	12m	19/01/2009
4	*HH* (FBS)	34.3°	Ascending / right looking	12m	17/02/2009

25 m for comparison with the polarimetric dataset. As the field size is more than 4–5 ha in most cases the resampling did not affect the classification performance significantly. The data were acquired over *rabi* cropping season when the predominant crops in the study area were wheat, mustard and gram.

Apart from crops two other landuse classes *viz.* bare soil and built-up area (or human settlements) that were present in the study area were also included for classification using SAR data. The full-polarimetric data over the area were acquired at an earlier date (Dec. 2008) compared to the single polarization acquisitions (Jan.–Feb. 2009) due to imaging constraints of ALOS-PALSAR. Ground truth information corresponding to the date of acquisitions of all the data were collected for subsequent crop analysis. Both the datasets, polarimetric and FBS were examined independently, thus no normalization was required.

3. METHODOLOGY

3.1. Synthesis of Circular and Hybrid Polarimetric Data from Linear Polarimetric SAR Data

As mentioned earlier, full-polarimetric radar data contains all the scattering information for any arbitrary polarization state (e.g., circular, linear and hybrid modes), hence data of any combination of transmit and receive polarizations can be synthesized, mathematically from linear fullpolarimetric data. A polarimetric SAR measures microwave reflectivity using quad-polarizations HH, HV, HV and VV to form a scattering matrix. For monostatic radar imaging of a reciprocal medium (where $HV = VH$), the three unique elements of the scattering vector is defined as:

$$\vec{k} = \begin{bmatrix} S_{HH} & \sqrt{2}S_{HV} & S_{VV} \end{bmatrix}^T \tag{1}$$

where the superscript 'T' denotes the matrix transpose. The $\sqrt{2}$ on the S_{HV} term is to ensure consistency in the span (total power) computation [28].

Compact or hybrid polarimetric SAR has been evolved as a substitute for full-polarimetric SAR in recent times as it offers a reduced complexity, cost, mass and data transmission rate of the SAR system while retaining full-polarimetric information of the target in the backscattered field. In compact polarimetric imaging mode the transmitter polarization is either circular (called CTRL Mode) or linear oriented at 45° (w.r.t the horizontal and vertical and called $\pi/4$ mode), and the receivers are either at horizontal (H) and vertical (V)

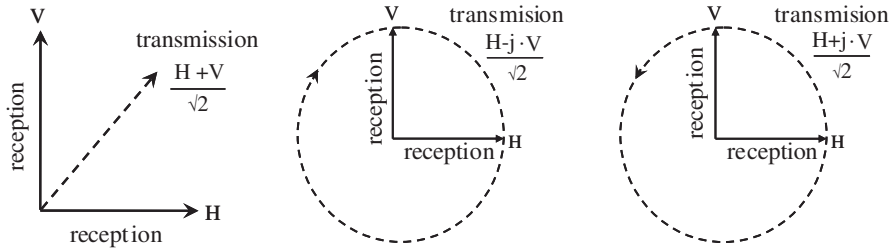

Figure 1. Schematic diagrams showing different hybrid polarimetric imaging modes where the transmission polarization is shown in dotted lines and reception polarizations are shown in solid lines. (a) $\pi/4$ mode. (b) Right circular hybrid mode. (c) Left circular hybrid mode.

polarizations or at right and left circular polarizations [21, 22, 25, 26]. This gives rise to various combinations of transmit and receive polarizations where a SAR system can be operated in the compact polarimetric imaging mode. Fig. 1 shows three possible modes of compact polarimetric imaging.

The circular and hybrid polarimetric data in different transmit — receive modes were synthesized from this linear polarimetric data as per the methods given below [1, 19, 21, 22, 26] in Table 2. SARSCAPE© software by SARMAP and PolSARPro© software by ESA for the synthesis and analysis of ALOS-PALSAR polarimetric SAR data have been used. (SARMAP and ESA) [4, 20].

3.2. Supervised Classification of Multi-polarization SAR Data

Supervised maximum likelihood (ML) classification algorithms based on Wishart distribution of complex polarimetric SAR data has been evaluated to assess the classification capabilities of multi-date, multi-polarization SAR data in dual, hybrid and quad-polarimetric modes over central state farm, Hisar with three crops and two other landuse classes. This classification technique has been selected as ground truth data for the training sites were available (Fig. 2(b)). The details of these classification algorithms can be found in literature [6, 10–15, 18]. We have however discussed the algorithm and methodology of the present classification in brief.

Most SAR data are multi-look processed for data volume compression and speckle reduction. The data are represented by a

Table 2. Polarization combinations and scattering vectors corresponding to various modes of operation of SAR in linear, circular as well as hybrid polarizations.

Mode	Polarization Combinations	Scattering Vector
Linear - Full	*HH, HV, V V*	$\vec{k}_{LIN} = \begin{bmatrix} S_{HH} \\ \sqrt{2}S_{HV} \\ S_{VV} \end{bmatrix}$
Circular - Full	*RR, RL, LL*	$\vec{k}_{CIR} = \begin{bmatrix} S_{RR} \\ \sqrt{2}S_{LR} \\ S_{LL} \end{bmatrix} = \frac{1}{2}\begin{bmatrix} S_{HH} - S_{VV} + i2S_{HV} \\ i(S_{HH} + S_{VV}) \\ S_{VV} - S_{HH} + i2S_{HV} \end{bmatrix}$
Circular - Dual	*RR, RL / LL, LR*	$\vec{k}_{RR,RL} = \frac{1}{\sqrt{2}}\begin{bmatrix} S_{HH} \pm S_{VV} \mp i2S_{HV} \\ i(S_{HH} + S_{VV}) \end{bmatrix}$
	RR, LL	$\vec{k}_{RR,LL} = \frac{1}{\sqrt{2}}\begin{bmatrix} S_{HH} - S_{VV} + i2S_{HV} \\ S_{VV} - S_{HH} + i2S_{HV} \end{bmatrix}$
Pi/4 Hybrid Mode	*π/4 H, π/4 V*	$\vec{k}_{\pi/4} = \frac{1}{\sqrt{2}}\begin{bmatrix} S_{HH} + S_{HV} \\ S_{VV} + S_{HV} \end{bmatrix}$
Right Circular Hybrid	*RH, RV*	$\vec{k}_{RCH} = \begin{bmatrix} RH \\ RV \end{bmatrix} = \frac{1}{\sqrt{2}}\begin{bmatrix} S_{HH} - iS_{HV} \\ -iS_{VV} + S_{HV} \end{bmatrix}$
Left Circular Hybrid	*LH, LV*	$\vec{k}_{LCH} = \begin{bmatrix} LH \\ LV \end{bmatrix} = \frac{1}{\sqrt{2}}\begin{bmatrix} S_{HH} + iS_{HV} \\ iS_{VV} + S_{HV} \end{bmatrix}$

polarimetric covariance matrix (Z) as:

$$Z = \frac{1}{n}\sum_{h=1}^{n} k(h)\cdot k(h)^{*T} = \begin{bmatrix} \left\langle |S_{HH}|^2 \right\rangle & \left\langle \sqrt{2}S_{HH}S_{HV}^* \right\rangle & \left\langle S_{HH}S_{VV}^* \right\rangle \\ \left\langle \sqrt{2}S_{HV}S_{HH}^* \right\rangle & \left\langle 2|S_{HV}|^2 \right\rangle & \left\langle \sqrt{2}S_{HV}S_{VV}^* \right\rangle \\ \left\langle S_{VV}S_{HH}^* \right\rangle & \left\langle \sqrt{2}S_{VV}S_{HV}^* \right\rangle & \left\langle |S_{VV}|^2 \right\rangle \end{bmatrix} \quad (2)$$

where the superscript '*' denotes complex conjugate; 'n' denotes number of looks and $< S >$ denote average of 'S' over 'n' samples.

The SAR polarimetric covariance matrix obeys the statistics of a complex multivariate Wishart distribution [12–14]. The probability

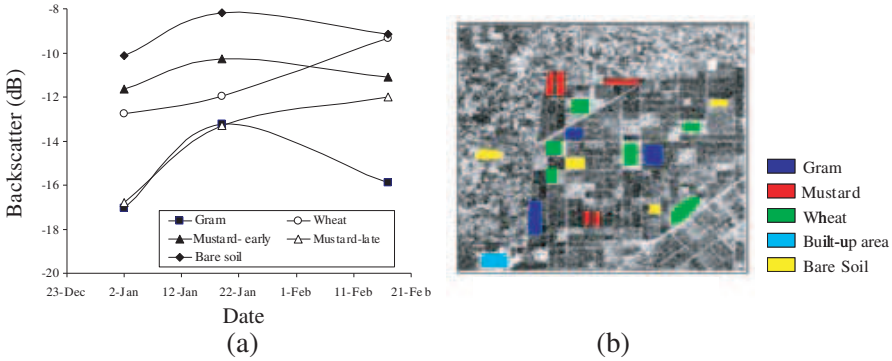

Figure 2. (a) Temporal profile of SAR backscatter in HH-polarization of major *rabi* crops in central state farm, Hisar, Haryana. (b) Ground truth map of major *rabi* crops in central state farm, Hisar, Haryana.

density function of the n-look covariance matrix, Z, is

$$p^{(n)}\left(Z|\,C\right) = \frac{n^{nq}\,|Z|^{n-q}\exp\left(-nTr\left(ZC^{-1}\right)\right)}{K\left(n,q\right)|C|^{n}} \tag{3}$$

where

$$C = E\left[Z\right],$$

'q' is the dimension of vector 'k' (here either 2 for dual-polarization case or 3 for reciprocal quad-polarization case),

'Tr' denotes the trace of a matrix, and $K(n,q)$ is the normalization constant; $K(n,q) = \pi^{\left(\frac{1}{2}\right)q(q-1)}\Gamma\left(n\right)\ldots\Gamma\left(n-q+1\right)$.

The ML classifier assigns a sample vector or matrix '$\underline{u}$' to the 'm' class, ω_m if

$$P\left(\underline{u}|\,\omega_m\right)P\left(\omega_m\right) > P\left(\underline{u}|\,\omega_j\right)P\left(\omega_j\right), \quad \text{for all } j \neq m \tag{4}$$

$P\left(\omega_m\right)$ is the *a priori* probability of class ω_m. In this application, the *a priori* probabilities are assumed to be equal. The above function of probability density function holds good for supervised maximum likelihood classification using threedate FBS HH data.

For landuse classification, a distance measure was derived based on the ML classifier (4) and the complex Wishart distribution (3)

$$d\left(Z,\omega_m\right) = \ln|C_m| + Tr\left(C_m^{-1}Z\right) \tag{5}$$

where $C_m = E\left[Z,\omega_m\right]$ is the mean covariance matrix of class ω_m. This distance measure is independent of the number of

looks, 'n'. Consequently, it can be applied to single-look, multi-look, and polarimetric speckle-filtered complex data. For supervised classification, training sets are required to estimate C_m for each class. The distance measure is then applied to classify each pixel.

Supervised Maximum Likelihood classification algorithms based on theoretical speckle distributions of multi-polarization and polarimetric SAR data has been used. Supervised classification was used, because unsupervised classification might have caused clusters to drift away from the class centers given by the user on the basis of ground truth data, and also because classes from the ground truth might not have corresponded to the cluster centers derived from the unsupervised segmentation. The multi-polarization and polarimetric data was filtered to reduce the effects of speckle on the classification results using a polarimetry preserving adaptive Enhanced Lee (3×3) filter [10]. Training site were selected corresponding to five land cover (three crops and two other) classes based on ground truth measurements and the image pixels were classified as one of the five fixed classes. Classification accuracy is assessed as the percentage of pixels correctly classified for each training area. The classification results and accuracy assessments are presented in the next section.

3.3. Supervised Classification of Multi-date Single Polarization SAR Data

The same methodology was followed for preprocessing and classification of multi-date single polarization SAR data. For single polarization data $q = 1$, which reduces (3) to the Chi-square distribution with $2n$ degree of freedom. Three date ALOS-PALSAR HH-polarization data over the study area were co-registered, speckle filtered and classified based on training sets from ground truth measurements. The ground truth samples are shown in Fig. 2(b). For supervised classification (using probability density function, algorithm sated above), the class mean values and the standard deviation of the ground truth points are considered. Around 50% of the points were used for building the supervised classification Algorithm and 50% kept for validating the post-classification results. The temporal variation of each landcover type has been captured in the model as manifested by the HH backscatter variation in the FBS data The crop growth is manifested in terms of increase in backscatter till January as shown in Fig. 2. In case of wheat and late sown mustard there is increase till February but decrease in some early sown mustard due to pod development and yellowing of leaves. This logic is captured from the ground truth data and classification has been performed based on the statistics of the training site.

The backscatter intensities (in logarithmic scale) of the data were computed as:

$$\sigma^0(\text{dB}) = 10 * \log_{10}(Intensity) + CF - 32.0 \quad (6)$$

where 'CF' is the calibration factor (here -83 dB) provided by JAXA for ALOS-PALSAR level 1.1 (SLC) products. Conversion of DN values to backscatter intensity after performing multilooking operation from the SLC data is shown in the above equation and $n = 4$.

4. RESULTS AND DISCUSSION

4.1. Temporal Variation of Backscatter and Crop Classification Using Multi-date Single-polarization SAR Data

Different crops are sown at different times and have different cropping practices and growth profiles. This makes crops separable in radar backscatter domain and this is the basis for crop discrimination and classification using multi-date SAR data. Fig. 2 shows the temporal variation of backscatter intensity for three crop types, i.e., gram, mustard, and wheat along with bare soil within the crop field. Here two classes of mustard, one early sown and other late sown have been depicted. L-band has greater penetration capability as compared to higher frequencies viz. X or C-band, in early crop stages or where the canopy is sparse (in case of gram) it picks up the soil information.

Mustard was the first crop to be sown in this region during early to mid October after the harvest of *Kharif* (summer) rice. It is a broad-leaved crop and has fast growth rate in the initial phase with peak vegetative phase occurring at mid January followed by flowering, podding (siliqua development) and maturity. Therefore the SAR backscatter values showed an increasing trend from October till January when the same for early-sown mustard variety saturated near the end of January with slight decline due to drooping habit due to the weight of the pods, backscatter decreases further due to leaf and pod yellowing. While for the late-sown variety continued to grow further and produced higher backscatter beyond January as depicted from Fig. 2. Gram was sown at a similar time as the mustard but unlike mustard its growth was quite slow resulting in exposure of bare soil most of the time of its growth cycle thus manifesting soil moisture and roughness variations Wheat was sown at a much later date (end of November to early December) in the study area and its vegetative growth continued during the SAR data acquisition period showing an increasing trend in backscatter. The backscatter contribution from bare soil remained high in the beginning and increased further till

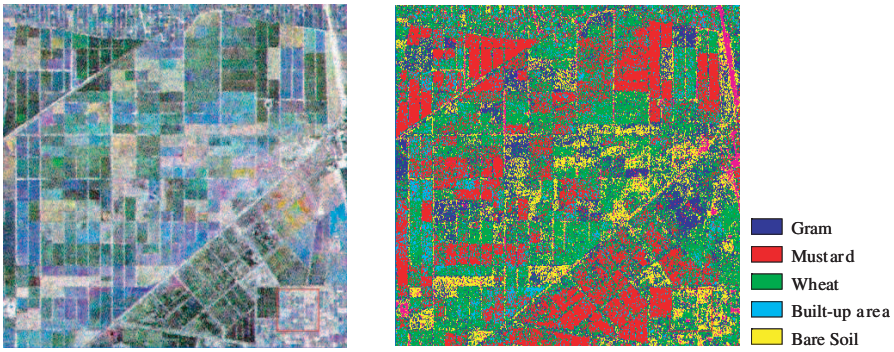

Figure 3. (a) FCC of 3 date (Jan. 2, Jan. 19 and Feb. 17, 2009) HH-polarization SAR data over central state farm, Hisar, Haryana. (b) Corresponding supervised classified image showing five landuse classes. The overall classification accuracy was 89.7% with a kappa coefficient of 0.85.

February due to the change in soil moisture regime with crop growth and declined thereafter with the growth in crop canopy. The soil moisture in this area changes with irrigation and was monitored. The area identified as fallow is rough as it is not irrigated thus giving high backscatter signature. In case of mustard full signature is captured as it is October sown Similar is the case with gram but as its canopy is slow growing and thus soil conditions underneath are manifested for a long time. But as roughness is less in the cropped field the backscatter is less as compared to rough fallow.

These variations in radar backscatter for different crop types over a time domain were utilized to classify crops and few other landuse classes using ALOS-PALSAR three-date HH-polarization SLC data. Fig. 3(a) shows the false colour composite (FCC) image generated by stacking co-registered HH-polarization SAR images of Jan. 2, Jan. 19, and Feb. 17, 2009 in RGB planes; and Fig. 3(b) shows the corresponding supervised classified image showing five landuse classes of a part of study area.

The efficiency of the classification (called classification accuracy) was calculated by summing the number of pixels classified correctly for all classes and dividing by the total number of pixels. The overall accuracy of the above classification was 89.7 % with kappa coefficient (which is another measure of classification accuracy, scaled from 0 to 1 [5] of 0.85.

4.2. Comparison of Crop Classification Using Different Modes of Single-date Multi-polarization SAR Data

Supervised classification of complex SAR data in different transmit and receive polarization combinations in linear, circular and hybrid polarimetric modes were conducted for three crops and two other landuse classes over central state farm. The training class separability (in backscatter domain) of the landuse classes in various polarization combinations are shown in Fig. 4. The scatter plots showed averaged training class cluster centers (in dB) are separable in various dual polarization data in linear, circular and hybrid modes. Fig. 5 shows the classified images of central state farm showing the above five landuse classes in various combinations of full-polarization, dual-polarization and hybrid polarization modes.

The classification accuracies of individual classes as well as of overall classifications along with corresponding 'kappa' coefficients; a measure of the efficiency of the classification process are shown in Table 3. The classification accuracies are shown in ascending order from top to bottom. The overall classification accuracy of the linear fullpolarimetric data was found to be highest among all, followed by circular quad and circular dual polarizations and then hybrid polarization combinations. The classification accuracies achieved by linear dual-polarization data was found to be lower than other dual polarization combinations in the present study.

The classification accuracy in full-polarimetric mode is higher due to higher dimensionality of data which contains complete co-

Table 3. Classification accuracies (overall) expressed in percent, of various crop and land cover classes as achieved through maximum likelihood distance measure method based supervised classification of ALOS PALSAR complex data at different polarization modes.

Polarization Combination	Gram	Mustard	Wheat	Built-up area	Bare Soil	Overall Accuracy (in %)	*Kappa Coeff.*
HH / HV	73.1	56.1	49.7	85.4	83.1	*71.8*	*0.63*
VH / VV	75.2	61.5	55.8	83.2	84.2	*73.0*	*0.65*
HH / VV	75.6	87.47	82.3	71.1	84.04	*77.5*	*0.71*
$\pi/4$ mode	63.8	85.9	73.5	85.2	87.0	*78.9*	*0.73*
RH / RV	71.9	86.9	82.1	86.1	80.2	*80.8*	*0.74*
LH / LV	69.2	85.9	80.3	88.3	90.7	*81.5*	*0.75*
RR / RL	80.0	87.4	94.4	87.8	85.1	*87.5*	*0.83*
LR / LL	79.6	89.3	94.2	90.8	94.7	*88.1*	*0.84*
RR / RL / LL	81.6	88.4	94.9	90.7	94.2	*89.7*	*0.86*
HH / HV / VV	91.1	87.9	97.7	91.1	93.2	*92.4*	*0.90*

polar and cross-polar scattering information. However, linear full-polarimetric data showed better overall classification accuracy (92.4%) than circular full-polarimetric data (89.7%). This can be explained through azimuthal symmetric conditions for natural targets [17].

Vegetation and other natural features are considered to be azimuthally symmetric but certain fields may exhibit azimuthally asymmetric polarimetric behaviour due to orientation of row crops along the radar line of sight, tillage patterns, lodging (by strong winds) or harvesting patterns [2, 8]. As circular polarization enforces symmetric condition of natural media, it resulted into slightly poorer crop discrimination in certain cases and subjected to misclassification where asymmetric conditions exist. In the study area bare soil, built-up area and mustard classes were symmetrical, resulting into the classification accuracies similar in linear as well as circular quad-polarization data. Whereas for wheat (grown in rows) and gram (asymmetric condition at early stage due to effect of tillage), the asymmetric conditions resulted into lower classification rate in circular polarimetric data than the linear full-polarimetric data.

Among the dual polarization data in linear, hybrid and circular modes, circular dual polarization modes produced highest overall classification accuracies (87.5% – 88%). The hybrid polarimetric modes data such as 'the $\pi/4$ mode' and 'circular transmit — linear orthogonal receive modes (CTLR)' showed intermediate classification accuracies (79%–81.5%). The linear dual-polarimetric modes data showed poorer classification accuracies compared to the other modes as shown in Table 3.

It should be noted that the different modes of hybrid polarimetric data originate from systems that transmit in a combination of horizontal and vertical polarizations and receive in either horizontal or vertical polarizations. For agricultural applications particularly crop discrimination the hybrid polarimetric modes act as quasi full-polarimetric that preserves more information about the target in the backscattered field compared to the linear dual-polarization modes. Circular dual-polarization mode is a special case of hybrid polarimetric mode where both the transmission and reception polarizations are combinations of 'horizontal' and 'vertical' polarizations. Also, the supervised classification algorithm used in the present study is based on the Wishart distance measure, which is statistical in nature. Speckle in polarimetric SAR data affect classification rates. The hybrid polarimetric data synthesized from linear polarimetric data are range and azimuth averaged. Such kind of averaging is commonly observed in all SAR data processing specially when SLC is converted to ground range image by multilooking. This process reduced speckle

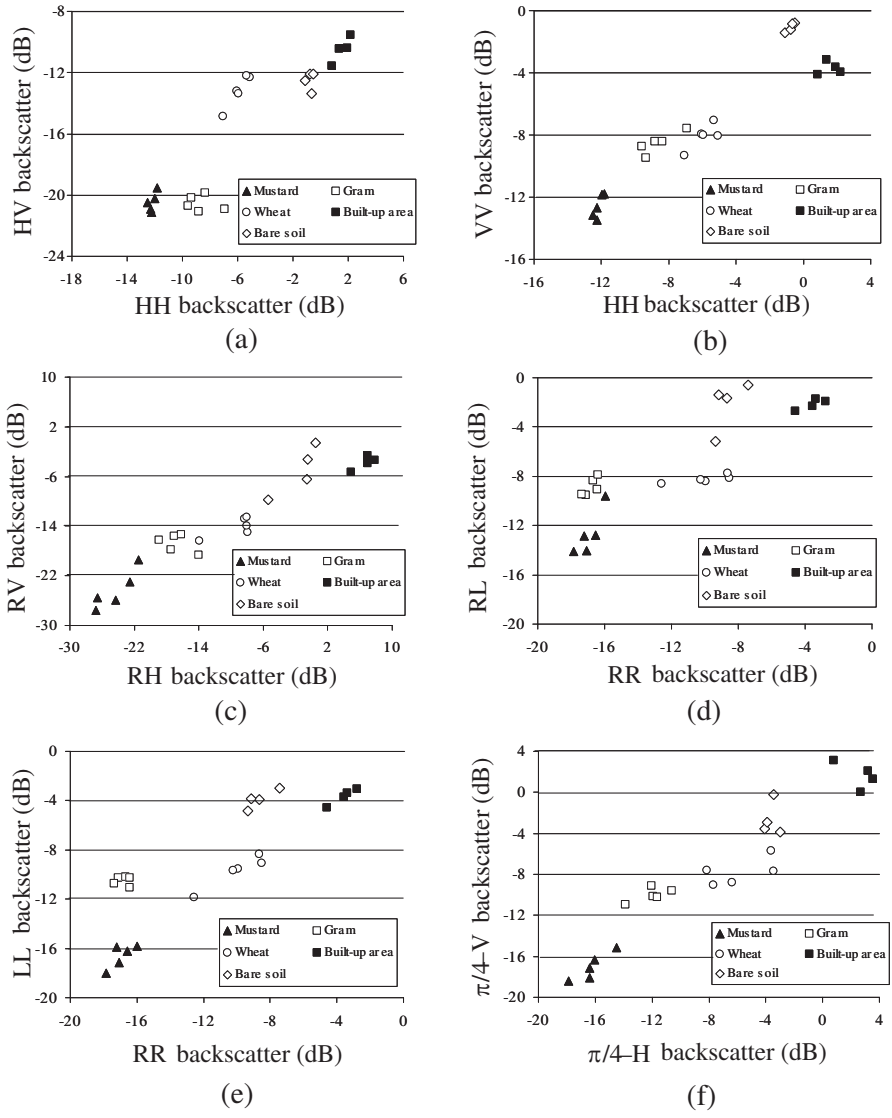

Figure 4. Training class separability of major rabi crops and other landuse classes in SAR backscatter data with different polarization combinations. (a) *HH-HV*. (b) *HH-VV*. (c) *RH-RV*. (d) *RR-RL*. (e) *RR-LL*. (f) $\pi/4H$-$\pi/4V$. Each marker represents the average value of a training class cluster.

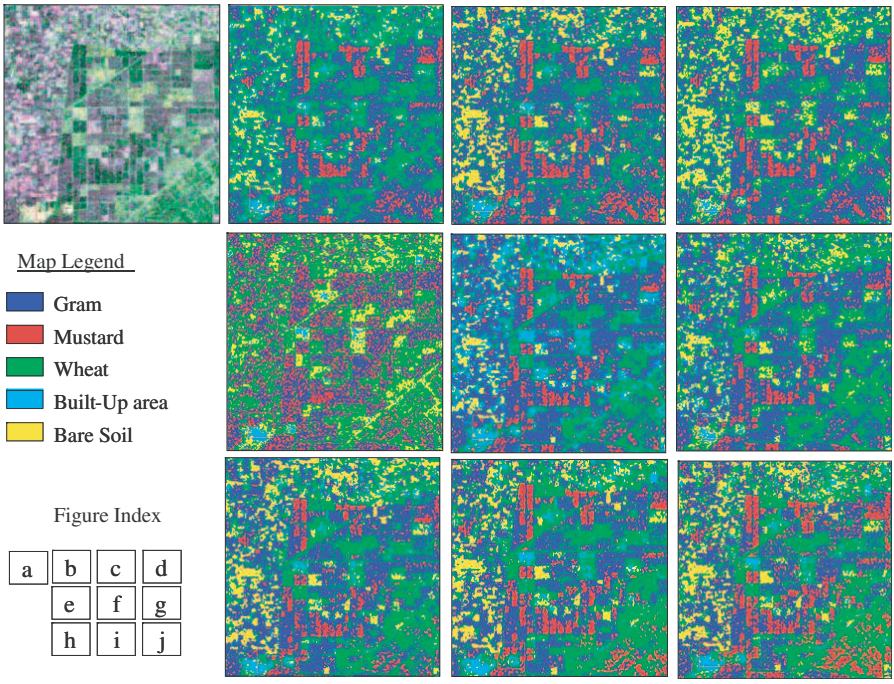

Figure 5. The quad-pol RGB image. (a) Corresponding classified images of central state farm, Hisar, Haryana during *rabi* season as derived from data of different polarization combinations. (b) HH/HV. (c) HV/VV. (d) HH/VV. (e) $\pi/4$ mode. (f) LH/LV. (g) RH/RV. (h) RR/RL. (I) $RR/RL/LL$. (j) $HH/HV/VV$.

in the hybrid polarimetric data. Thus, small fluctuations in the cluster statistics resulted within individual classes due to speckle are minimized in hybrid polarimetric data resulting in higher classification accuracies. The speckle filter used in both the cases is enhanced Lee filter of window size 3×3.

Among the linear dual-polarization modes, complex co-polarization data (HH-VV) showed higher classification accuracies than the complex cross-polarization data (HH-HV or VV-VH) in L-band as shown in Table 3. This may be attributed to a meaningful polarization phase difference between HH and VV which is an important factor for crop classification particularly for a relatively advanced stage crop like Mustard (LAI around 2 or more). The phase difference between co-polarization and cross-polarization terms are not as important as that between HH and VV, because co-polarization and

cross-polarization terms are generally uncorrelated in distributed targets. This is in agreement with the results published earlier by various authors [13, 26].

The above study showed that although hybrid polarimetric data do not produce as good classification accuracies as produced by full-polarimetric data, hybrid polarimetric data with circular polarization transmit and linear polarization receive mode has great potential for polarimetric SAR applications as it provides a simplistic SAR hardware configuration yet much superior than the dual polarized SAR in terms of target information content. The classification results were also compared with the same derived from multi-date single polarization data and it was observed that multi-polarization data produced similar or better crop and other landuse classification accuracy. Thus, single-date full-polarimetric data can serve as a substitute for multi-date single polarization data and this can also help in forecasting crop area and hence crop production at an earlier date.

5. CONCLUSIONS

Single date fullpolarimetric SAR data in L-band gave comparable or higher crop classification accuracy than three date single polarization (HH) SAR data in the central state farm, Hisar, Haryana. Thus, single-date full-polarimetric data can serve as a substitute for multi-date single polarization data and this can also help in forecasting crop area and hence crop production at an earlier date. As the field size is more than $4,5$ ha in most cases the resampling did not affect the classification performance significantly. We studied crop and other landuse classification accuracies using L-band polarimetric SAR data of different polarization combinations in linear circular and hybrid modes and observed that full-polarimetric data produced highest classification rates followed by hybrid dual-polarization data which was again followed by linear dual-polarization data. Circular polarization data provided similar accuracy as linear polarization data, but the latter is more desirable for crop discrimination. Among the linear dual-polarization combinations HH-VV polarization combination produced better crop discrimination and hence crop classification results than HH-HV or VV-VH polarization combinations due to the importance of co-polarization phase difference in crop classification. Hybrid polarization modes showed almost similar classification accuracies with CTLR mode found to be slightly better than $\pi/4$ mode. If multitemporal full-polarimetric data is available some improvement is expected as compared to the single date polarimetric data. It is evidenced by a parallel study carried out by the author using Radarsat2

data for the current year.

The study demonstrated the capabilities of multi-polarization SAR data for crop and other landuse classifications in L-band. The hybrid polarization data in different modes were found to be good for crop classifications but they do not substitute full-polarimetric data as full-polarimetric data produces highest classification accuracy for crops and other landuse classes.

ACKNOWLEDGMENT

Authors are thankful to Dr. R. R. Navalgund, Director, Space Applications Centre for his support and guidance to carry out the present work. Authors would like to thank Japan Aerospace Exploration Agency (JAXA), Japan for providing ALOS PALSAR data under ALOS R.A. project. The authors are also grateful to Dr. J. S. Parihar, Dy Director, Earth, Ocean, Atmosphere, Planetary Sciences and Applications Area (EPSA) for his constant encouragements and valuable suggestions.

REFERENCES

1. Ainsworth, T. L., J. P. Kelly, and J.-S. Lee, "Classification comparisons between dual-pol, compact polarimetric and quad-pol SAR imagery," *ISPRS Journal of Photogrammetry and Remote Sensing*, Vol. 64, 464–471, 2009.
2. Bouman, B. A. M. and D. H. Hoekman, "Multi-temporal, multi-frequency radar measurements of agricultural crops during the Agriscatt-88 campaign in the Netherlands," *International Journal of Remote Sensing*, Vol. 14, 1595–1614, 1993.
3. Ballester-Berman, J. D. and J. M. Lopez-Sanchez, "Time series of hybrid-polarity parameters over agricultural crops," *Geoscience and Remote Sensing Letters*, in press, 2011.
4. ENVI and SARSCAPE ver 4.2 2009 ITT Visual Information Solutions. SARscape is a Registered Trademark of Sarmap s.a. Switzerland.
5. Foody, G. M., "Status of landcover classification accuracy assessment," *Remote Sensing of Environment*, Vol. 80, 185–201, 2002.
6. Ferro-Famil, L., E. Pottier, and J. S. Lee, "Unsupervised classification of multifrequency and fully polarimetric SAR images based on the H/A/Alpha — Wishart classifier," *IEEE*

Transactions on Geoscience and Remote Sensing, Vol. 39, No. 11, 2332–2341, 2001.

7. Freeman, J., J. D. Villasenor, H. P. Klein, and J. Groot, "On the use of multi-frequency and polarimetric radar backscatter features for classification of agricultural crops," *Int. J. Remote Sensing*, Vol. 15, No. 9, 1799–1812, 1994.
8. Hoekman, D. H. and B. A. M. Bouman, "Interpretation of C- and X-band radar images over an agricultural area, the flevoland test site in the agriscatt-87 campaign," *International Journal of Remote Sensing*, Vol. 14, 1577–1594, 1993.
9. Lavalle, M., D. Solimini, E. Pottier, and Y.-L. Desnos, "Compact polarimetric radar interferometry," *IET Radar Sonar Navig.*, Vol. 4, No. 3, 449–456, 2010.
10. Lee, J. S., M. R. Grunes, and G. De Grandi, "Polarmetric SAR speckle filtering and its implication on classification," *IEEE Trans. Geosci. Remote Sensing*, Vol. 37, 290–301, 1999b.
11. Lee, J. S., K. W. Hoppel, S. A. Mango, and A. R.Miller, "Intensity and phase statistics of multilook polarimetric and interferometric SAR imagery," *IEEE Trans. Geosci. Remote Sensing*, Vol. 32, 1017–1028, 1994b.
12. Lee, J.-S., M. R. Grunes, and R. Kwok, "Classification of multi-look polarimetric SAR imagery based on complex wishart distributions," *International Journal of Remote Sensing*, Vol. 15, No. 11, 2299–231, 1994.
13. Lee, J.-S., M. R. Grunes, and E. Pottier, "Quantitative comparison of classification capability: Fully polarimetric versus dual-and single-polarization SAR," *IEEE Transactions on Geoscience and Remote Sensing*, Vol. 39, No. 11, 2343–2351, 2001.
14. Lee, J.-S., M. R. Grunes, T. L. Ainsworth, L. J. Du, D. L. Schuler, and S. R. Cloude, "Unsupervised classification using polarimetric decompositions and the complex wishart classifier," *IEEE Transactions on Geoscience and Remote Sensing*, Vol. 37, No. 5, 2249–2258, 1999.
15. Lim, H. H., "Classification of earth terrain using polarimetric SAR images," *J. Geophys. Res.*, Vol. 94, 7049–7057, 1989.
16. Mishra, P., D. Singh, and Y. Yamaguchi, "Landcover classification of PALSAR images," *Progress In Electromagnetic Research*, Vol. 30, 47–70, 2011.
17. Nghiem, S. V., S. H. Yueh, R. Kwok, and F. K. Li, "Symmetry properties in polarimetric remote sensing," *Radio Science*, Vol. 27, No. 5, 693–711, 1992.

18. Nielsen, A. A., H. Skriver, and K. Conradsen, "Complex wishart distribution based analysis of polarimetric synthetic aperture radar data," *IEEE Symposium Proceedings*, 1–6, 2007.
19. Nord, M., T. L. Ainsworth, J.-S. Lee, and N. Stacy, "Comparison of compact polarimetric synthetic aperture radar modes," *IEEE Transactions on Geoscience and Remote Sensing*, Vol. 47, No. 1, 174–188, 2009.
20. "Recent advances in development of the open source tool box for polarimetric and interferometric polarimetric SAR data processing," The Polsarpro v 4.1.5. Eric Pottier IETR UMR CNRS 6164. Univ. of Rennes. SAPHIR Team, Rennes, France.
21. Raney, R. K., "Dual-polarized SAR and stokes parameters," *IEEE Geoscience and Remote Sensing Letters*, Vol. 3, No. 3, 317–319, 2006.
22. Raney, R. K., "Hybrid-polarity SAR architecture," *IEEE Transactions on Geoscience and Remote Sensing*, Vol. 45, No. 1, 3397–3404, 2007.
23. Schotten, C. G. J., W. W. L. Van Rooy, and L. L. F. Janssen, "Assessment of the capabilities of multi-temporal ERS-1 SAR data to discriminate between agricultural crops," *Int. J. Remote Sensing*, Vol. 16, No. 14, 2619–2637, 1995.
24. Skriver, H., T. S. Morten, and A. G. Thomsen, "Multitemporal C- and L-band polarimetric signatures of crops," *IEEE Transactions on Geoscience and Remote Sensing*, Vol. 37, No. 5, 2413–2429, 1999.
25. Souyris, J. C. and S. Mingot, "Polarimetry based on one transmitting and two receiving polarizations: the $\pi/4$ mode," *Proc. IGARSS*, 4, Toronto, Canada, 2002.
26. Souyris, J. C., P. Imbo, R. Fjortoft, S. Mingot, and J. S. Lee, "Compact polarimetry based on symmetry properties of geophysical media: the $\pi/4$ mode," *IEEE Transactions on Geoscience and Remote Sensing*, Vol. 43, No. 3, 634–646, 2005.
27. Stacy, N. and M. Preiss, "Compact polarimetric analysis of X-band SAR data," *In. Proceedings of EUSAR*, 4, Dresden, May 16–18, 2006 (on CDROM).
28. Boerner, W. M., et al., "Polarimetry in radar remote sensing: Basic and applied concepts," *Principles and Applications of Imaging Radar, The Manual of Remote Sensing*, 3rd edition, Ch. 5, Wiley, New York, 1998.